Research Article | Vol. 6, No. 9 | 1 Sep 2016 | OPTICAL MATERIALS EXPRESS 2871

Optical Materials EXPRESS

Effect of lithium excess on the $LiAl_5O_8$:Eu luminescent properties under VUV excitation

VERÔNICA C. TEIXEIRA,[1,*] LUCAS C. V. RODRIGUES,[2] DOUGLAS GALANTE,[1] AND MARCOS V. dos S. REZENDE[3]

[1]*Laboratório Nacional de Luz Síncrotron, Centro Nacional de Pesquisa em Energia e Materiais, 13084-971 Campinas, SP, Brazil*
[2]*Departamento de Química Fundamental, Instituto de Química, Universidade de São Paulo, Av. Prof. Lineu Prestes, 748, 05508-000, São Paulo, SP, Brazil*
[3]*Grupo de Nanomateriais Funcionais (GNF), Departamento de Física, Universidade Federal de Sergipe, 49500-000, Itabaiana, SE, Brazil*
[*]*veronica.teixeira@lnls.br*

Abstract: The influence of lithium excess and calcination temperature on the luminescence properties of the $LiAl_5O_8$:Eu under VUV excitation was investigated. The presence of both broad bands and sharp peaks in the VUV and X-ray emission spectra suggests the presence of Eu^{2+}, even in absence of reducing atmosphere in the synthesis. The VUV excitation spectra indicated a band gap of 8.5 eV while the UV excited one showed the Eu^{3+} charge transfer transition starting at 3.9 eV. These values indicate that Eu^{2+} is stable in this host since its ground state is below the Fermi level of the host (*ca.* 4.1 eV). The relation between the intensity of Eu^{2+} and Eu^{3+} emissions showed that the reduction is favored at higher temperatures and lower Li content, leading to the proposition of a reduction mechanism based on the incorporation of charge compensation defects formed in the aliovalent doping of Eu^{3+} in Li^{+} sites.

OCIS codes: (300.6280) Spectroscopy, fluorescence and luminescence; (160.2540) Fluorescent and luminescent materials; (160.5690) Rare-earth-doped materials; (250.5230) Photoluminescence; (260.3800) Luminescence; (260.7210) Ultraviolet, vacuum; (340.6720) Synchrotron radiation.

References and links

1. V. Singh and T. K. Gundu Rao, "Studies of defects in combustion synthesized europium-doped $LiAl_5O_8$ red phosphor," J. Solid State Chem. **181**(6), 1387–1392 (2008).
2. S. S. Pitale, V. Kumar, I. M. Nagpure, O. M. Ntwaeaborwa, E. Coetsee, and H. C. Swart, "Cathodoluminescent properties and surface characterization of bluish-white $LiAl_5O_8$:Tb phosphor," J. Appl. Phys. **109**(1), 013105 (2011).
3. R. T. Wegh, H. Donker, A. Meijerink, R. J. Lamminmäki, and J. Hölsä, "Vacuum-ultraviolet spectroscopy and quantum cutting for Gd^{3+} in $LiYF_4$," Phys. Rev. B **56**(21), 13841–13848 (1997).
4. D. Wang, Y. Wang, and L. Wang, "Photoluminescence properties of $Sr(Y, Gd)_2O_4$:Eu^{3+} under VUV excitation," J. Lumin. **126**(1), 135–138 (2007).
5. P. Dorenbos, "The 5d level positions of the trivalent lanthanides in inorganic compounds," J. Lumin. **91**(3-4), 155–176 (2000).
6. P. K. Sharma, R. K. Dutta, and A. C. Pandey, "Performance of YAG:Eu^{3+}, YAG:Tb^{3+} and BAM:Eu^{2+} plasma display nanophosphors," J. Nanopart. Res. **14**(3), 731 (2012).
7. J. T. Ingle, A. B. Gawande, R. P. Sonekar, P. A. Nagpure, and S. K. Omanwar, "Synthesis and photoluminescence of inorganic borate host red emitting VUV phosphor $YCaBO_4$:Eu^{3+}," AIP Conf. Proc. **1536**, 895–896 (2013).
8. T. Abritta and F. S. Barros, "Luminescence and photoacoustic measurements of $LiAl_5O_8$: Fe^{3+}," J. Lumin. **40–41**, 187–188 (1988).
9. S. C. Bhargava, "Spin-lattice relaxation of Fe^{3+} ions in $LiAl_5O_8$," J. Phys. C Solid State Phys. **19**(35), 7045–7070 (1986).
10. V. Singh, R. P. S. Chakradhar, J. L. Rao, and D. K. Kim, "EPR and luminescence properties of combustion synthesized $LiAl_5O_8$:Mn phosphors," Mater. Chem. Phys. **110**(1), 43–51 (2008).
11. V. Singh, R. P. S. Chakradhar, J. L. Rao, and H. Y. Kwak, "Characterization, EPR and photoluminescence studies of $LiAl_5O_8$:Cr phosphors," Solid State Sci. **11**(4), 870–874 (2009).
12. T. R. N. Kutty and M. Nayak, "Cationic distribution and its influence on the luminescent properties of Fe^{3+}-doped $LiAl_5O_8$ prepared by wet chemical methods," J. Alloys Compd. **269**(1-2), 75–87 (1998).
13. X. Duan and D. Yuan, "Synthesis and characterization of Co^{2+}-doped lithium aluminum spinel nanocrystals," J. Non-Cryst. Solids **351**(27-29), 2348–2351 (2005).

#266672 http://dx.doi.org/10.1364/OME.6.002871
Journal © 2016 Received 19 May 2016; revised 24 Jun 2016; accepted 24 Jun 2016; published 11 Aug 2016

Optical Materials EXPRESS

14. A. P. Jadhav, Amol Pawar, U. Pal, B.K. Kim, and Y.S. Kang, "Synthesis of Monodispersed Red Emitting $LiAl_5O_8$: Fe^{3+} Nanophosphors," Sci. Adv. Mater. **4**(5–6), 597–603 (2012).
15. S. S. Pitale, V. Kumar, I. Nagpure, O. M. Ntwaeaborwa, and H. C. Swart, "Luminescence investigations on $LiAl_5O_8$:Tb^{3+} nanocrystalline phosphors," Curr. Appl. Phys. **11**(3), 341–345 (2011).
16. O. A. Lopez, J. McKittrick, and L. E. Shea, "Fluorescence properties of polycrystalline Tm^{3+}-activated $Y_3Al_5O_{12}$ and Tm^{3+}-Li^+ co-activated $Y_3Al_5O_{12}$ in the visible and near IR ranges," J. Lumin. **71**(1), 1–11 (1997).
17. Y. Guo, D. Wang, and F. Wang, "Effect of Li^+ ions doping on microstructure and upconversion luminescence of CeO_2: Er^{3+} translucent ceramics," Opt. Mater. **42**, 390–393 (2015).
18. H. Jin, H. Wu, and L. Tian, "Improved luminescence of Y_2MoO_6:Eu^{3+} by doping Li^+ ions for light-emitting diode applications," J. Lumin. **132**(5), 1188–1191 (2012).
19. Q. Du, G. Zhou, J. Zhou, X. Jia, and H. Zhou, "Enhanced luminescence of novel $Y_2Zr_2O_7$:Dy^{3+} phosphors by Li^+ co-doping," J. Alloys Compd. **552**, 152–156 (2013).
20. O. Kaygili, S. Keser, R. H. Al Orainy, T. Ates, and F. Yakuphanoglu, "In vitro characterization of polyvinyl alcohol assisted hydroxyapatite derived by sol-gel method," Mater. Sci. Eng. C **35**, 239–244 (2014).
21. M. Sivakumar, S. Kanagesan, R. Suresh Babu, S. Jesurani, R. Velmurugan, C. Thirupathi, and T. Kalaivani, "Synthesis of $CoFe_2O_4$ powder via PVA assisted sol–gel process," J. Mater. Sci. Mater. Electron. **23**(5), 1045–1049 (2012).
22. R. L. Cavasso-Filho, M. G. P. Homem, R. Landers, and A. N. Brito, "Advances on the Brazilian toroidal grating monochromator (TGM) beamline," J. Electron Spectrosc. Relat. Phenom. **144–147**, 1125–1127 (2005).
23. R. L. Cavasso-Filho, A. F. Lago, M. G. P. Homem, S. Pilling, and A. N. Brito, "Delivering high-purity vacuum ultraviolet photons at the Brazilian toroidal grating monochromator (TGM) beamline," J. Electron Spectrosc. Relat. Phenom. **156–158**, 168–171 (2007).
24. L. C. V. Rodrigues, R. Stefani, H. F. Brito, M. C. F. C. Felinto, J. Hölsä, M. Lastusaari, T. Laamanen, and M. Malkamäki, "Thermoluminescence and synchrotron radiation studies on the persistent luminescence of $BaAl_2O_4$:Eu^{2+}, Dy^{3+}," J. Solid State Chem. **183**(10), 2365–2371 (2010).
25. D. Dutczak, T. Jüstel, C. Ronda, and A. Meijerink, "Eu($^{2+}$) luminescence in strontium aluminates," Phys. Chem. Chem. Phys. **17**(23), 15236–15249 (2015).
26. R. Famery, F. Queyroux, J.-C. Gilles, and P. Herpin, "Etude structurale de la forme ordonnée de $LiAl_5O_8$," J. Solid State Chem. **30**(2), 257–263 (1979).
27. R. D. Shannon, "Revised effective ionic radii and systematic studies of interatomic distances in halides and chalcogenides," Acta Crystallogr. A **32**(5), 751–767 (1976).
28. H. L. Yakel, "A refinement of the crystal structure of monoclinic europium sesquioxide," Acta Crystallogr. B **35**(3), 564–569 (1979).
29. P. Dorenbos, "Systematic behaviour in trivalent lanthanide charge transfer energies," J. Phys. Condens. Matter **15**(49), 8417–8434 (2003).
30. L. van Pieterson, M. F. Reid, R. T. Wegh, S. Soverna, and A. Meijerink, "$4f^n \rightarrow 4f^{n-1}$ 5d transitions of the light lanthanides: Experiment and theory," Phys. Rev. B **65**(4), 045113 (2002).
31. I. Veljković, D. Poleti, L. J. Karanović, M. Zdujić, and G. Branković, "Solid state synthesis of extra phase-pure $Li_4Ti_5O_{12}$ spinel," Sci. Sinter. **43**(3), 343–351 (2011).
32. P. Dorenbos, "Absolute location of lanthanide energy levels and the performance of phosphors," J. Lumin. **122–123**, 315–317 (2007).
33. P. Dorenbos, "Locating lanthanide impurity levels in the forbidden band of host crystals," J. Lumin. **108**(1–4), 301–305 (2004).
34. V. Kumar, A. F. Khan, and S. Chawla, "Intense red-emitting multi-rare-earth doped nanoparticles of YVO_4 for spectrum conversion towards improved energy harvesting by solar cells," J. Phys. D Appl. Phys. **46**(36), 365101 (2013).
35. S. Emura, H. Maeda, and M. Nomura, "Variation of optical luminescence X-ray excitation spectra," Phys. B Condens. Matter. **208–209**, 108–110 (1995).
36. P. Strobel, J. J. Capponi, C. Chaillout, M. Marezio, and J. L. Tholence, "Variations of stoichiometry and cell symmetry in $YBa_2Cu_3O_{7-x}$ with temperature and oxygen pressure," Nature **327**(6120), 306–308 (1987).
37. P. G. Radaelli, J. D. Jorgensen, A. J. Schultz, J. L. Peng, and R. L. Greene, "Evidence of apical oxygen in Nd_2CuO_y determined by single-crystal neutron diffraction," Phys. Rev. B Condens. Matter **49**(21), 15322–15326 (1994).
38. L. C. V. Rodrigues, J. Hölsä, H. F. Brito, M. Maryško, J. R. Matos, P. Paturi, R. V. Rodrigues, and M. Lastusaari, "Magneto-optical studies of valence instability in europium and terbium phosphors," J. Lumin. **170**, 701–706 (2016).

1. Introduction

Luminescent properties of rare-earth doped oxides, carbides and/or sulfides, under vacuum ultraviolet (VUV) excitation, have attracted a considerable attention due the possibility of their application in mercury-free fluorescent lamps, photoluminescence liquid crystal display (PLLCD) [1], field emission displays (FED) [2] and plasma display panels (PDPs) [3–5]. For PDP, for example, many of the phosphors commercially available, as the red ones, have poor chromaticity and low efficiency under VUV excitation (λ< 200 nm), mainly in the range between 146 and 173 nm, which correspond to the emission range from the inert gas plasma

Optical Materials EXPRESS

used for building PDPs [6,7]. Therefore, there is a current demand for the development of new materials with high efficiency, as well as a better understanding of their luminescence mechanisms when they are excited in the VUV range. Doped lithium aluminates ($LiAl_5O_8$ - LAO) are among the candidates for this kind of application as cited on the literature [8–15]. For example, LAO doped with Eu^{3+} has demonstrated its potential to be applied as a phosphor for use in PLLCD due to its orange red/red emission [1] and LAO: Tb^{3+} was also cited as a bluish-white phosphor able to be applied in FED, cathode X-ray tube and fluorescent devices [2].

High luminescence efficiency is a property, which can be strongly influenced for many factors such as annealing temperatures, particles size and structural composition. Several studies show that the addition of Li^+ as co-dopant in different materials can be used to enhance their luminescence emission [16–19]. Some authors reported that Li^+ ions improved the crystallinity, changed the grain size and also contributed to the creation of oxygen vacancies [16,19]. In this work, we report the effects of Li^+ excess and calcination temperature on the $LiAl_5O_8$:Eu luminescent properties, when exposed to VUV radiation. The application of this system a potential new red VUV phosphor for PDP is discussed.

2. Experimental

LAO phosphors were doped with 3 mol% Eu, stoichiometric prepared and also with 0.5 mol% of Li excess. The chemical method for getting the samples was the sol-gel based on polyvinyl alcohol (PVA) [20,21] and the starting reactants were the metal nitrates $LiNO_3$ (99.99%), $Al(NO_3)_3$ (99.9%) and $Eu(NO_3)_3$(99.99%), all from *Sigma*-Aldrich and a PVA solution (0.1 g/ml). The raw materials, in stoichiometric amounts, were dissolved in distilled water and then 30% of PVA was added based on the final volume of the starting solution. The system was kept under stirring at constant temperature of 100 °C during 4 h. Finally, the obtained dried gels, or xerogels, were calcined in static air at 900 and 1000 °C for 2 h.

The crystal structure and phase purity of the $LiAl_5O_8$:Eu materials were routinely verified with the X-ray powder diffraction (XRD) measurements using a Rigaku RINT 2000/PC diffractometer with Co-Kα radiation (1,79 Å), in the Bragg-Brentano geometry. The VUV excitation of integrated luminescence and the photoluminescence (PL) emission spectra were recorded at room temperature and in ultra-high vacuum (better than 10^{-7} mTorr) conditions at the Toroidal Grating Monochromator (TGM) beamline (E/ΔE ~500 to 700) of the Brazilian Synchrotron Light Laboratory (LNLS) [22, 23], which was recently upgraded and now covers from 3 to 330 eV. Monochromatic photons from 6 – 10 eV (~206 to 124 nm), filtered using a MgF_2 (thickness: 200 μm) window, were used for exciting the samples and the emitted light was collected by an optical fiber (aperture: 600 μm) coupled to the chamber by a vacuum feedthrough and connected to a R928 Hamamatsu photomultiplier (PMT). In front of the PMT, a glass slide (thickness: 170 μm) was used for cutting the scattered light (λ<300 nm), in a setup prepared to collect the total photoluminescence yield (TPY) of the sample. The photoluminescence emission spectra were recorded for specific energies (6.5 and 8.5 eV – 191 and 146 nm, respectively) and the setup was composed by an optical fiber connected to an Ocean Optics QE65000 spectrometer. The spectra were corrected for the variation in the incident flux of the excitation beam using the excitation and emission spectra of sodium salicylate ($C_7H_5NaO_3$) as standard [24, 25]. The UV excitation spectra were recorded using a spectrofluorometer Fluorolog 3 from Horiba at the Advanced Optical Spectroscopy Multiuser Laboratory from the Institute of Chemistry from the University of Campinas (FAPESP/LMEOA/IQ/UNICAMP). The total X-ray Excited Optical Luminescence (XEOL) yield was registered, around the Al K edge and the XEOL emission spectra were recorded at the Soft X-ray Spectroscopy (SXS) beamline at the LNLS using a similar setup to the TPY measurements, but exciting the samples with X-rays (1566 eV, above the Al K edge).

3. Results and discussion

The XRD patterns (Fig. 1) exhibit only the reflection peaks of the spinel structure of the $LiAl_5O_8$ with the $P4_332$ (or $P4_132$) space group [26]. No clear effect in the crystalline

Optical Materials EXPRESS

structure or secondary phase was observed with the Li^{+} excess, Eu^{3+} doping or different calcination temperatures. In $LiAl_5O_8$, there are one tetrahedral (8c) and two (distorted) octahedral (4b and 12d) sites. It is known that Al^{3+} occupies both tetrahedral and octahedral sites (preferentially 12d), while Li^{+} occupies only the distorted octahedral ones (preferentially 4b) [26]. The Eu^{3+} ions cannot occupy the tetrahedral site, but can substitute either the Al^{3+} or Li^{+} octahedral sites. However, the smaller ionic radius of Al^{3+} (0.535 Å) compared to Li^{+} (0.76 Å) and Eu^{3+} (0.94 Å), all with coordination number VI [27], suggests that Eu^{3+} will more probably substitute Li^{+}, requiring a charge compensation. Furthermore, the average Al-O distance in the 12d site is 1.90 Å while the Li-O in 4b is 2.05, closer to the average Eu-O distance in the Eu_2O_3 sesquioxide, ranging from 2.2 to 2.7 Å [28].

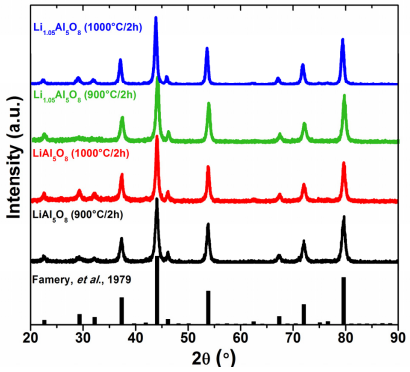

Fig. 1. XRD patterns of the $Li_{1+x}Al_5O_8$:Eu (x = 0 and 0.05) materials compared to the standard structure proposed by Famery *et al*., (1979) [26].

The VUV excitation spectra of the emission of $LiAl_5O_8$:Eu materials (Fig. 2) exhibit a broad band at *ca.* 191 nm and a sharp edge at *ca.*150 nm. The edge close to 150 nm (8.3 eV) is related to transitions from the top of the valence band (VB) to the bottom of the conduction band (CB), *i.e.* the host band gap or the formation of free electron-hole pair. The band gap energy (E_g) can be estimated using the minima of the first derivative of the excitation spectra, which is at 150 nm. The differences in the E_g as a function of synthesis temperature or the excess of Li^{+} (ranging from 150.0 to 150.6 nm) are smaller than the resolution of the TGM beamline (+/– 2 nm at the measurements energy range).

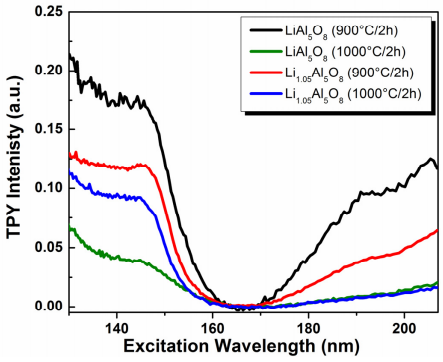

Fig. 2. Excitation spectra for $LiAl_5O_8$:Eu total luminescence yield scanned at the VUV range.

The second band, with maxima at 190 and 205 nm, is associated to the O(2p)→Eu^{3+} charge transfer excitation of Eu^{3+} ions. This band starts at 320 (3.9 eV) in the UV region with maximum at 255 nm (Fig. 3) and continue to the VUV region. The lowest energy of this band is compatible to the Eu-O CT band in other Eu^{3+} doped oxide and aluminate hosts, which starts normally at 4-6 eV [29]. Since the VUV excitation spectra (Fig. 2) takes into account

Optical Materials EXPRESS

the integrated emission, it is also probable that the Eu^{2+} $4f^7 \rightarrow 4f^6 5d^1$ excitation bands are overlapped in this region. On the other hand, it is not probable that this band arises from Eu^{3+} $4f^6 \rightarrow 4f^5 5d^1$ excitation since the energy of these transitions should occur only at higher energies than 8.5 eV (<140 nm) [5,30], which were avoided with the use of the MgF_2 filter.

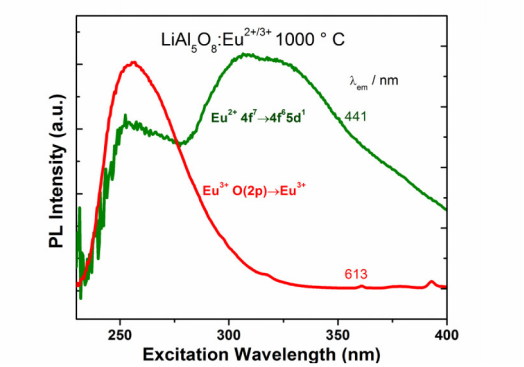

Fig. 3. PL excitation spectra of $LiAl_5O_8$:Eu, calcined at 1000°C, monitoring the Eu^{2+} (441 nm) (green curve) and Eu^{3+} (613 nm) (red curve) emission wavelength.

In order to investigate the relationships between the lithium excess and calcination temperature on the luminescent properties of $LiAl_5O_8$:Eu under VUV excitation, the emission spectra of $LiAl_5O_8$:Eu and $Li_{1.05}Al_5O_8$: Eu, calcined at 900 and 1000°C, were measured under excitation below (191 nm) and above (146 nm) the band gap, as shown in Fig. 4.

The emission spectra under excitation at the Eu^{3+} CT band (191 nm) of $LiAl_5O_8$:Eu and $Li_{1.05}Al_5O_8$:Eu samples exhibit two broad bands centered at 300 and 480 nm and peaks at 612 and 700 nm (Fig. 4, left). All the spectra were normalized in intensity to the $^5D_0 \rightarrow {}^7F_2$ transition of Eu^{3+} at 612 nm. The band at 300 nm probably arises from defects' emission. Several defects can be present in this host as intrinsic Schottky ones generated via evaporation of the volatile Li_2O [31] or those created by the charge compensation needed when doping a trivalent ion (Eu^{3+}) in a monovalent site (Li^+).

The peaks at the range of 585 to 750 nm are due to Eu^{3+} emission from the excited state $^5D_0$ to the ^7F_J (J: 0-4). Finally, the 480 nm band arises probably from the allowed $4f^6 5d^1 \rightarrow 4f^7$ emission of Eu^{2+} ions, formed due to the high temperature synthesis. Eu^{2+} can be stable at very high Fermi energy materials, which seems to be the case of LAO. The Fermi energy is normally half of the gap energy [32], in this case *ca.* 4.1 eV. The energy of Eu^{2+} ground state can be estimated using the energy of the Ligand to Metal Charge Transfer (LMCT) $O(2p) \rightarrow Eu^{3+}$ transition [33] which starts at 3.9 eV in this host. Eu^{2+} is, thus, stable in this host since its ground state is below the Fermi energy. Albeit the Eu^{2+} concentration being very small, its allowed transition facilitates its identification by the analysis of the emission spectra, even if not detectable by X-ray absorption spectroscopy. Even if the emission probability of Eu^{2+} (Laporte allowed) is much higher than Eu^{3+} one (Laporte forbidden), under very low Eu^{2+} concentrations a comparison between the emission ratio of Eu^{2+}/Eu^{3+} in different spectra can qualitatively indicate an increase/decrease in the reduction process. Thus, the higher Eu^{2+}/Eu^{3+} emission ratio increase under higher calcination temperatures indicate that the reduction is a temperature-dependent reaction.

The emission spectra measured with excitation above the band gap at 146 nm (Fig. 4, right) exhibit the same bands of the spectra of LMCT excited, with an extra peak at 710 nm. This peak is related to Cr^{3+} ruby like $^2E \rightarrow {}^4A_2$ emission. Most of Al reactants contain Cr^{3+} as an impurity and this peak is similar to the one observed by Singh et. al. for the Cr^{3+} doped lithium aluminate[11]. This result show that there is no energy transfer from Eu^{3+} to Cr^{3+}, since, when excited in the Eu^{3+} LMCT energy (Fig. 4, left), no Cr^{3+} emission is observed.

Optical Materials EXPRESS

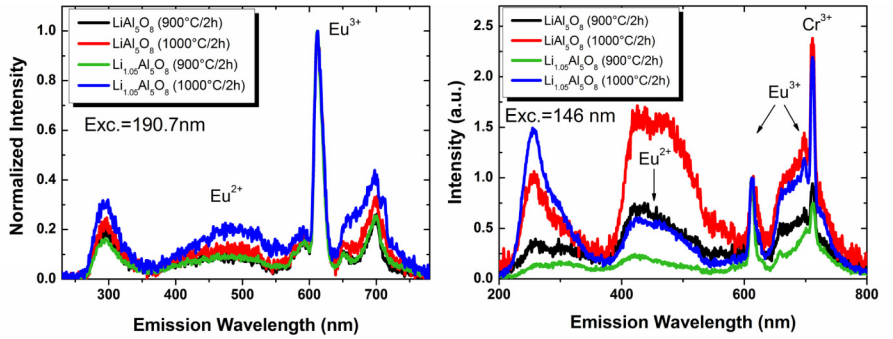

Fig. 4. PL emission spectra of $LiAl_5O_8$:Eu and $Li_{1.05}Al_5O_8$:Eu samples excited at 191 nm (left) and 146 nm (right). All spectra were normalized to the Eu^{3+} $^5D_0 \rightarrow {}^7F_2$ transition intensity.

Differently from the CT excited, the emission spectra excited above band gap energy (Fig. 4, right) exhibit more intense Eu^{2+} bands, allowing a better understanding of the reduction mechanism. Most of the red emitting PDP materials found in literature have an emission at only the red region [34], thus we show a new possibility of PDP materials that may be tuned from red to blue emission depending on excitation wavelength and synthesis parameters.

One can observe that the ratio of Eu^{2+}/Eu^{3+} emissions increases with temperature, and decreases with excess of Li^+. As already pointed out, Li_2O is a volatile oxide, so the effect of temperature might be related to the lack of Li^+ in the system. Besides, the changes in the optical properties of the solids with different Li concentration cannot be related to Li^+ itself since Li^+ ($1s^2$) is optically inactive and thus the only optical properties changes caused by its excess are related to the changes on $Eu^{2+/3+}$ stabilization.

Both excitations (190 and 147 nm) promote Eu^{2+} as well as Eu^{3+} to excited states, allowing both Laporte allowed and forbidden radiative emissions, respectively. The 190 excitation allows Eu^{2+} emission because in this region, $4f^7 \rightarrow 4f^6 5d^1$ transition is overlapped to the Eu^{3+} LMCT band, as it can be observed in conventional excitation spectroscopy in the UV region (Fig. 3). On the other hand, the reason that 147 nm excitation allows both emissions is due to the formation of electron-hole pair followed by an energy transfer for both ions. To confirm this mechanism for excitation at high energy, the total XEOL yield was registered (Fig. 5, left) showing that the luminescence increases as a function of excitation energy and around the Al K edge it presents a positive edge. It suggests there is very efficient energy transference originated from the recombination of electron-holes pairs that excites the material's optical channels [35]. The XEOL emission spectra (Fig. 5, right) exhibited the same profile as the band gap excited spectra, presenting defects and Eu^{2+} bands, as well as the Eu^{3+} and Cr^{3+} peaks. This result confirms that once the electrons are excited to very high energy states, the energy is transferred to all emitting centers.

A model that explains how the two valences of Eu ions are actually accommodated inside the $LiAl_5O_8$ structure is based on the charge compensation defects, which are created in the aliovalent substitution of Li^+ by Eu^{3+}. The trivalent Eu^{3+} ions doped into $LiAl_5O_{12}$ will replace the Li^+ ions due to size similarity, forming the positive defect $Eu_{Li}^{\bullet\bullet}$ and interstitial oxide ions O_i'' (Eq. (1)). It is well known that interstitial oxide ions can be oxidized to $O_2(g)$ at high temperatures reducing other species like Cu^{2+} in superconductors [36,37] or Eu^{3+} in persistent luminescence materials [24] (Eq. (2)). This oxidation will be more spontaneous at higher temperatures, which explains the higher amount of Eu^{2+} in the 1000 °C heated samples.

Optical Materials EXPRESS

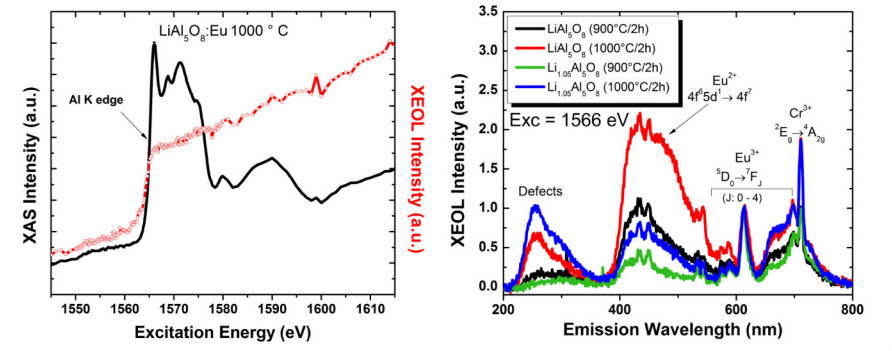

Fig. 5. Total XEOL yield and excitation spectra (left) and XEOL emission spectra (right) of $LiAl_5O_8$:Eu and $Li_{1.05}Al_5O_8$:Eu samples.

The electrons released in the interstitial oxide oxidation reduce the $Eu_{Li}^{\cdot\cdot}$ species to $Eu_{Li}^{\cdot}$ (Eq. (3)). Since Eu^{2+} has a larger ionic radius (1.17Å) compared to Eu^{3+} (0.95Å) and Li^{+} (0.76Å), it will be better accommodated if there is more space for distortions, like in the presence of Li vacancies. It means that the samples heated at 1000 °C will accommodate better the Eu^{2+} ions due to the evaporation of Li_2O be more effective at higher temperatures. The lack of Li will also be higher in the stoichiometric samples corroborating with the results from emission spectroscopy. The presence of defects (e.g. $V_{Li}^{'}$) was demonstrated by the use of synchrotron radiation, both in the VUV and X-ray around de Al K edge for exciting the samples, which resulted in the presence of luminescence in the UV region at the emission spectra. Unfortunately, the exact origin of these defects is hard to know.

$$Li_{Li}^{\times} \rightarrow Eu_{Li}^{\cdot\cdot} + O_i^{''} \quad (1)$$

$$2O_i^{''} \rightarrow O_2(g) + 4e^{'} \quad (2)$$

$$Eu_{Li}^{\cdot\cdot} + e^{'} \rightarrow Eu_{Li}^{\cdot} \quad (3)$$

Based on our data, it is difficult to give a quantitative amount of Eu^{2+} and Eu^{3+} ions from the emission intensities of the sample because the two luminescence centers have their own characteristic excitation wavelengths. For example, Eu^{2+} has a Laporte-allowed, spin-forbidden transition with lifetime of the order of μs, while Eu^{3+} has a Laporte-forbidden transition with lifetime of the order of ms. This difference allows energy transfer from Eu^{2+} to Eu^{3+} that can increase Eu^{3+} emission instead of its expected decrease as it is reduced to Eu^{2+}. The determination of their concentrations could be better accomplished with X-ray absorption or even paramagnetic susceptibility [38] measurements, that will be done in future works.

4. Conclusions

The influence of lithium excess and calcination temperature on the luminescence properties of the $LiAl_5O_8$:Eu under VUV excitation is related to the higher $Eu^{3+} \rightarrow Eu^{2+}$ reduction in the stoichiometric and at higher calcination temperatures. This reduction occurs due to the necessary charge compensation when Eu^{3+} substitutes the monovalent Li^{+} ion. The emission of defects under VUV and X-ray excitation corroborates the presence of these charge compensation defects. The presence of divalent europium is proved with both VUV-excited emission and UV excitation spectra which are composed by Eu^{2+} and Eu^{3+} ions transitions. The VUV excitation measurements yielded the value of the host band gap (8.3 eV), indicating that the Fermi level of the system is above Eu^{2+} ground state. The tuning of luminescence of this material may be done by changing the amount of Li and calcination temperature, making this a promising system for application as green/red VUV phosphor.

Optical Materials EXPRESS

Funding

FAPESP; FINEP; CAPES; CNPq (No. 470.972/2013-0).

Acknowledgments

The authors thank the FAPESP/LMEOA/IQ-UNICAMP and the TGM (Internal Research) and SXS (Proposal #19076) beamlines from the Brazilian Synchrotron Light Laboratory (LNLS) from the Brazilian Center for Research in Energy and Materials (CNPEM).